Magnetic and transport properties in layered $Nd_{1-x}Sr_{1+x}CoO_4$

Shengli Huang, Keqing Ruan,* Zhangming Lv, Lihui Zhuang, Peng Wei, Huiyan Wu, Mi Li, Junliang Zhang, Yisheng Chai, Hongshun Yang, Liezhao Cao, and Xiaoguang Li

Structure Research Laboratory and Department of Physics, University of Science and Technology of China, Hefei, Anhui 230026, P. R. China

(Received 13 September 2005; revised manuscript received 21 November 2005; published 22 March 2006)

Electrical resistance, thermoelectric power, dc magnetization, ac susceptibility, and electron spin resonance (ESR) are investigated for the polycrystalline $Nd_{1-x}Sr_{1+x}CoO_4$ ($x=0.25$, 0.33, and 0.60). Powder x-ray diffraction (XRD) confirms that these compounds crystallize in K_2NiF_4-type structure with space group I4/mmm. The specimens exhibit ferromagnetic and semiconducting behaviors. With Sr doping, the lattice parameter c increases, the cusp intensity related to spin-glass states weakens, and the ferromagnetic property intensifies. The transport mechanisms in high temperature range obey Arrhenius law and might be understood by small polaron models. The magnetic properties present spin-glass states at ~18 K and Griffiths singularity at ~210 K.

DOI: 10.1103/PhysRevB.73.094431 PACS number(s): 75.50.Pp, 76.30.Fc, 75.50.Lk, 61.10.Nz

I. INTRODUCTION

The discovery of high temperature superconductivity and colossal magnetoresistance has aroused extended interest in the magnetic and electrical properties of perovskite transition metal oxides. The layered-type perovskite oxides A_2BO_4 with a K_2NiF_4-type structure is the two-dimensional confinement of the B-O-B network that significantly reduces the one-electron band width of the e_g electrons, thus induces strong electron correlation and alters the degrees of freedom (charge, spin, orbital, and lattice). Lots of intriguing physical properties have been discovered in the transition-metal oxides with this kind of structure, such as spin-state transition in $La_{2-x}Sr_xCoO_4$,[1] small polaron models in $La_{1.85-x}Sr_{0.15+x}Cu_{1-x}Fe_xO_4$,[2] spin-glass states in $La_{2-x}Sr_xCoO_4$,[1] and $La_{1-x}Sr_{1+x}MnO_4$,[3] orbital ordering in $La_{0.5}Sr_{1.5}MnO_4$,[4] charge ordering in $La_{1-x}Sr_{1+x}MnO_4$,[4] $La_{1.5}Sr_{0.5}CoO_4$,[5] and $(La,Sr)_2NiO_4$,[6] and high-temperature superconductivity in $La_{2-x}Sr_xCuO_4$. Up to now, compounds in K_2NiF_4 structure of copper-oxides, manganese-oxides, and nickel-oxides have been thoroughly studied. But for $Nd_{1-x}Sr_{1+x}CoO_4$, except the structure for $0\leqslant x\leqslant 0.3$,[7,8] infrared character for $0\leqslant x\leqslant 0.3$,[8] and electrical resistance and magnetization for $x\leqslant 1.0$,[9,10] little is known so far about the properties in the relatively higher doping range $0\leqslant x\leqslant 1$. Here we investigate the magnetic and transport properties in $Nd_{1-x}Sr_{1+x}CoO_4$ ($x=0.25$, 0.33, and 0.60) and show how the properties evolve with Sr doping. Existence of the small polarons, spin-glass states and Griffiths singularity in the material will also be discussed.

II. EXPERIMENTAL

The bulks $Nd_{1-x}Sr_{1+x}CoO_4$ with $x=0.25$, 0.33, and 0.60 were prepared by decomposing the nitrates mixture in KNO_3.[7] The sintered pellets were further annealed at 750 °C for 36 h in O_2 atmosphere. The samples with sufficient oxygen content and a high density were obtained. Structure and phase purity of the samples were checked by powder x-ray diffraction (XRD) at room temperature. Electrical resistance and Seebeck coefficients were measured from 20 to 300 K with home-built apparatuses, which include a four-probe device for the former and the equipment as described in Ref. 11 for the latter. DC magnetization and ac susceptibility measurements were carried out in a superconducting quantum interference device (SQUID) magnetometer. The dc magnetization was measured from 5 to 300 K in an applied field of 1000 Oe. In the zero-field-cooling (ZFC) measurements the samples were cooled down from room temperature to 5 K before the measured field was applied. In the field-cooling (FC) measurements the samples were cooled in the applied field from room temperature to 5 K. The ac susceptibility was measured from 2 to 40 K in a driving field of amplitude $H_0=1000$ Oe at different frequency as well as at a frequency 80 Hz in different H_0. All the magnetic data $M_{ZFC}(T)$, $M_{FC}(T)$, $\chi'(T)$, and $\chi''(T)$ were collected in warming the samples up. Electron-spin-resonance (ESR) measurements were performed using a JES-FA200 spectrometer, operating at 9.067 GHz, with scanning field 0–800 mT in the temperature range 110–300 K.

III. RESULTS AND DISCUSSION

As seen in Fig. 1, the powder XRD patterns of $Nd_{1-x}Sr_{1+x}CoO_4$ with $x=0.25$, 0.33, and 0.60 are fully indexed as the tetragonal K_2NiF_4 structure (space group: I4/mmm).[7] No impurity phase is observed in the specimens. Table I gives the lattice parameters a and c. With increasing Sr content, the a parameter changes very little while the c parameter increases clearly. The results are in good agreement with those reported in the literatures[7,8] and can be ascribed to the substitution of the smaller size Nd^{3+} ion by the considerably larger size Sr^{2+} ion and the oxidization of Co^{3+} (low spin and high spin) to Co^{4+} (high spin).

Figure 2 shows the temperature dependence of resistivity for $Nd_{1-x}Sr_{1+x}CoO_4$. The specimens exhibit semiconducting like behavior over all the temperature ranges measured. At room temperature the resistivity ρ_r increases with increasing x. Figure 3 shows the temperature dependence of thermoelectric power (S) in $Nd_{1-x}Sr_xCoO_4$. The S decreases with

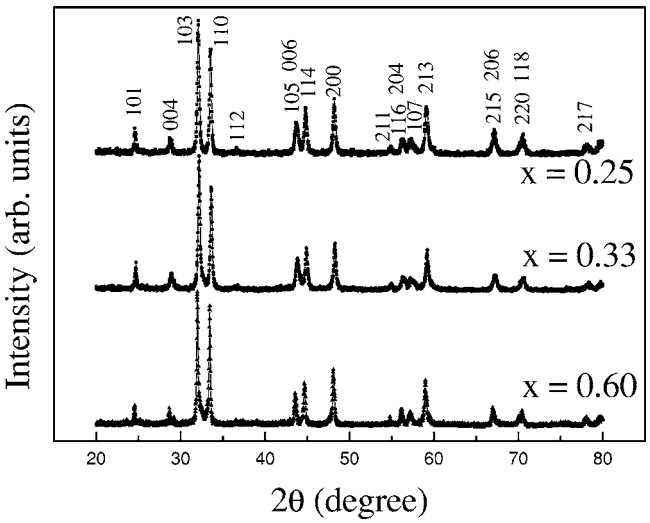

FIG. 1. Powder x-ray diffraction patterns of $Nd_{1-x}Sr_{1+x}CoO_4$ at room temperature.

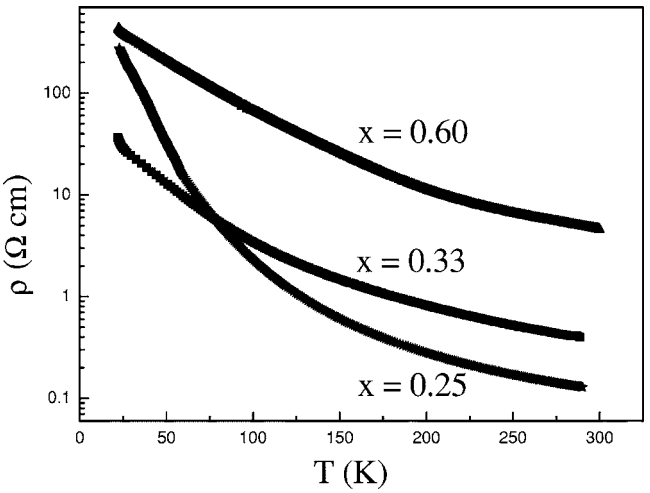

FIG. 2. Resistivity vs temperature for $Nd_{1-x}Sr_{1+x}CoO_4$.

decreasing temperature for each specimen, and displays a relatively weak temperature dependence in $x=0.60$. For $x=0.25$ and 0.33 S is positive in the whole temperature range, indicating p-type conduction in these compounds. However, for $x=0.60$ S changes from positive to negative around 60 K as shown in the inset, which suggests competing carriers or scattering mechanisms resulting in partial thermoelectric power.

For the three specimens the data show that the resistivity and thermoelectric power at high temperatures follow an Arrhenius law, i.e., thermally activated (intrinsic) conduction:

$$\rho(T) = \rho_0 \exp(\epsilon/k_B T) \quad \text{and} \quad S(T) = \pm (K_B/e)(\epsilon/k_B T + A).$$

Where the + and − signs hold for hole-type and electron-type of conduction, and the constant A is determined by the energy dependence of the scattering time.[2,12] Figure 4 displays the variation of $\ln \rho$ and S as a function of $1/T$ for $Nd_{1-x}Sr_{1+x}CoO_4$. The activation energy ϵ derived from the slope of straight lines at high temperature ($T > T_0$) is summarized in Table I. Here, ϵ_ρ and ϵ_s denote the activation energy derived from resistivity and thermoelectric power, respectively. The analysis of the activation energy shows that a great difference between ϵ_ρ and ϵ_s exists for the material. Similar results are also obtained in the experiment on thin film with $x=0.25$ (In the ab plane of the thin film, $\epsilon_\rho = 64.67$ meV and $\epsilon_s = 2.78$ meV. Detailed experiments and physical properties of the film will be discussed elsewhere.), which rules out the contribution from grain boundaries in polycrystals that increase the electrical resistance and in turn affect the intrinsic activation energy. As suggested in $La_{1.85-x}Sr_{0.15+x}Cu_{1-x}Co_xO_y$,[12] this discrepancy might be understood in terms of small polaron models, the self-localized states which are induced by the magnetic coupling between magnetic ions and hole spins. The polaron formation energy ϵ_P can be explained as $\epsilon_P = 2(\epsilon_\rho - \epsilon_s)$.

TABLE I. Variation of the lattice parameters a and c, temperature range ($T > T_0$), activation energy ϵ_ρ and ϵ_s, Curie temperature T_C, and bifurcating temperature T_B as a function of hole content x in $Nd_{1-x}Sr_{1+x}CoO_4$ system.

Doping	$X=0.25$	$X=0.33$	$X=0.60$
a (A)	3.769±0.001	3.774±0.001	3.776±0.001
c (A)	12.367±0.001	12.379±0.001	12.388±0.001
T_0 (K)	114	148	136
ϵ_ρ (meV)	40.19	35.86	43.97
ϵ_s (meV)	2.65	2.68	1.26
T_C (K)	179.0	185.7	193.3
T_B (K)	162.5	186.5	195.6

Figure 5 shows the temperature dependence of FC and ZFC magnetizations and inverse susceptibilities in $Nd_{1-x}Sr_{1+x}CoO_4$. At high temperature the $M_{FC}(T)$ and $M_{ZFC}(T)$ curves are substantially identical for each specimen, so we only considered the $M_{ZFC}(T)$ curve in this temperature range. In Figs. 5(a) and 5(b), $M_{FC}(T)$ and $M_{ZFC}(T)$ increase firstly with increasing temperature. Both show a cusp structure at ~18 K. Then $M_{ZFC}(T)$ increases continuously and shows a broad maximum at ~80 K while $M_{FC}(T)$ decreases slowly in the same temperature range. After that, both $M_{FC}(T)$ and $M_{ZFC}(T)$ decrease steeply until they combine each other at ~190 K, which indicates a phase change from a ferromagnetic to paramagnetic state.

From these curves several features and four critical temperatures could be distinguished: (i) The cusp structure in $M(T)$ at $T_{SG} \sim 18$ K, which was also observed in $La_{2-x}Sr_xCoO_4$ ($x=0.4$ and 0.6)[1] at $T_{SG} \sim 20$ K, $La_{0.92}Sr_{0.08}CoO_3$[13] at $T_{SG}=24$ K, as well as $La_{1-x}Sr_{1+x}MnO_4$[3] at $T_{SG}=20-25$ K, suggests a spin-glass transition. The intensity of the cusp decreases with Sr doping. Other experiments on the both single crystalline and polycrystalline samples of Sr_2CoO_4 and $Sr_{2-x}Y_xCoO_4$[9,10] showed no cusp structure in magnetization curve. The results denote that the substitution of Nd^{3+} by Sr^{2+} can reduce the disorder of the spin system. (ii) An anomalous change presents in susceptibility at $T_G \sim 210$ K that separates the two Curie-Weiss temperature do-

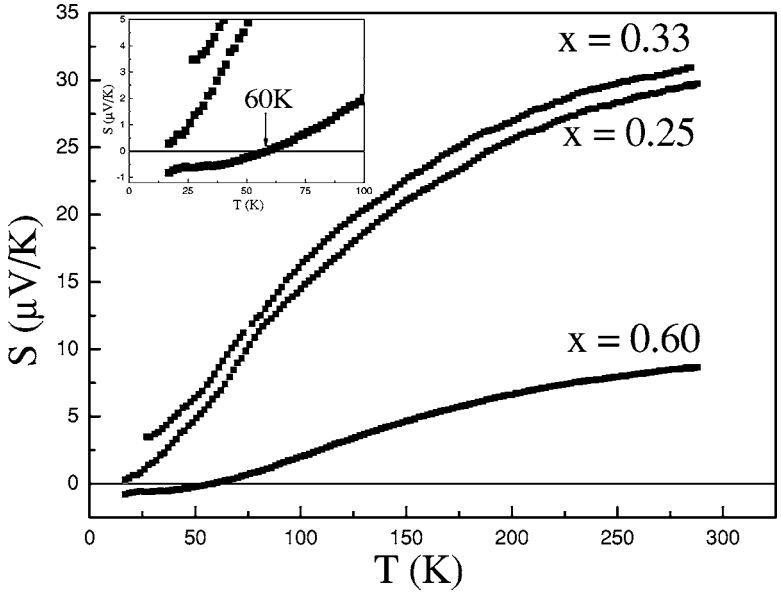

FIG. 3. Thermoelectric power vs temperature for $Nd_{1-x}Sr_{1+x}CoO_4$. (The magnifying graphs of S at low temperature are shown in the inset.)

mains as shown in Fig. 5(d) and the inset. As discussion followed the anomalism could be due to the presence of Griffiths singularity, i.e., the formation of short-range ferromagnetic clusters with larger spins in the paramagnetic matrix. Such Griffiths singularity are also observed at $T_G \sim 220$ K for $(La_{1-x}Y_x)_{2/3}Ca_{1/3}MnO_3$[14] and ~ 100 K for $Rb_2Co_{1-x}Mn_xF_4$.[15] (iii) The Curie temperature T_C and the temperature T_B at which $M_{FC}(T)$ and $M_{ZFC}(T)$ curves bifurcate, increase with Sr doping as shown in Table I. Here, we denote T_C as the intersecting point between the least-square-fitted straight line of $1/\chi_{ZFC}(T)$ below T_G and x-coordinate. The feature implies that the substitution can strengthen the ferromagnetic property for the material.

The presence of spin-glass states in $Nd_{1-x}Sr_{1+x}CoO_4$ was well confirmed by ac susceptibility on the sample with $x=0.25$. In Fig. 6, a peak emerges around T_{SG} in both in-phase and out-of-phase components of ac susceptibility. The peak is dependent on frequency and shifts to higher temperature monotonously when the frequency increases from 10 to 1000 Hz in the ac driving field of amplitude $H_0=1000$ Oe [see Figs. 6(a) and 6(b)]. Moreover, the peak is depressed continuously when H_0 increases from 700 to 2000 Oe at a frequency $f=80$ Hz [see Figs. 6(c) and 6(d)]. Such a behavior is the typical features of conventional spin-glass systems.[16] For the material there are ferromagnetic double-exchange interactions between Co^{3+}-Co^{4+} and antiferromagnetic superexchange interactions between Co^{3+}-Co^{3+} and Co^{4+}-Co^{4+}. It may be the competition between the ferromagnetic and antiferromagnetic interactions along with randomness at T_{SG} that causes the spin-glass behavior.

To explore the magnetic order further we performed ESR measurements on $Nd_{0.75}Sr_{1.25}CoO_4$ in the temperature range 110–300 K. In Fig. 7, at high temperature a signal (called "A signal") presents and is well fitted by the derivative of Dysonian function consisting of two terms.[17] The signal broadens and wipes out when the temperature decreases. While another signal (called "B signal") appears at lower resonant field and intensifies with temperature decreasing. Because both the signals appear mostly in different magnetic region, the A signal can be attributed to an ordinary paramagnetic resonance while the B signal is a ferromagnetic resonance originating from intergrowths of other parasitic phases undergoing ferromagnetic transition. The most important feature of the graph is that the ESR signals change drastically near Curie temperature ($150\ \text{K} < T < 190\ \text{K}$) due to paramagnetic and ferromagnetic states transition. While at paramagnetic state ($T \geqslant 190$ K) or ferromagnetic state ($T \leqslant 150$ K) the ESR signals change very little. The results indicate that near T_C (as shown in Table I, $T_C=179$ K), the ferromagnetic clusters present in the paramagnetic phase, and similarly, the paramagnetic elements present in the ferromagnetic phase. Both of them compete with each other severely around T_C.

Figure 8 shows the temperature dependence of the resonant field H_r, peak-to-peak line width ΔH_{pp}, and intensity I about the A signal. The intensity was calculated by $I=Y'_{max} \times (\Delta H_{pp})^2$, where Y'_{max} corresponding to the peak-to-peak amplitude of the measured derivative signal. It is noteworthy that all the parameters show a discontinuity near T_G, just the anomalism point in the paramagnetic range of dc susceptibil-

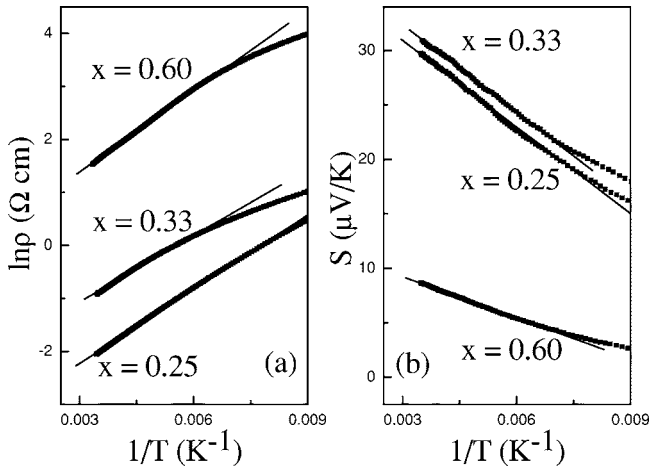

FIG. 4. ln ρ and S as a function of $1/T$ for $Nd_{1-x}Sr_{1+x}CoO_4$.

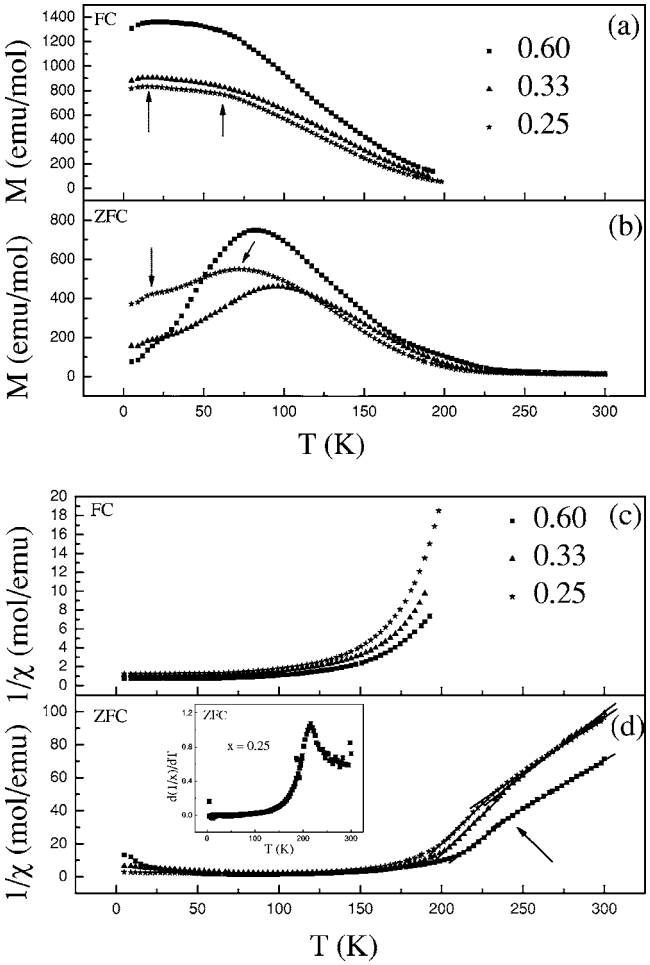

FIG. 5. Temperature dependence of the magnetizations and inverse susceptibilities for $Nd_{1-x}Sr_{1+x}CoO_4$. (a) and (b): FC and ZFC magnetizations. (c) and (d): FC and ZFC inverse susceptibilities. Inset: The $d(1/\chi)/dT$ as a function of temperature in $Nd_{0.75}Sr_{1.25}CoO_4$.

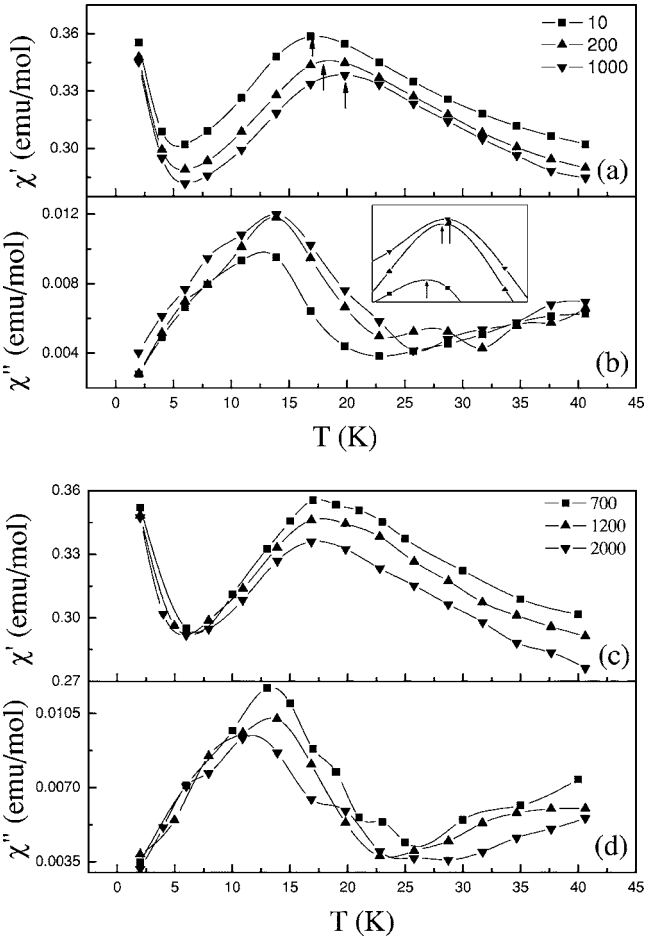

FIG. 6. Temperature dependence of the ac susceptibility for $Nd_{0.75}Sr_{1.25}CoO_4$. (a) and (b): In-phase $\chi'(T)$ and out-of-phase $\chi''(T)$ components with an ac driving field of amplitude H_0 = 1000 Oe oscillating at different frequency, 10, 200, and 1000 Hz. (c) and (d): In-phase $\chi'(T)$ and out-of-phase $\chi''(T)$ components with H_0=700, 1200, 2000 Oe oscillating at a frequency of 80 Hz. The arrows in (b) and the inset indicate the temperatures of the peaks.

ity, which suggests that this may be an intrinsic phenomenon for the material. Moreover, the intensity appears a maximum at T_c. The g factor, calculated by $g=h\nu/\beta H_r$, changes from 2.837 at T=160 K to 2.057 at T=280 K. In contrast with the free electron g factor g_e=2.0023, the higher g values suggest the intense orbital-spin correlation in the material.

Because the anomalism point emerges nearly in the same temperature point as the materials that have a uniform structure, $La_{1-x}Sr_{1+x}MnO_4$[3] and $(La,Sr)_2NiO_4$,[6] one may assumed that all of them would origin from the same mechanism, i.e., charge ordering. However, in this way transfer of a hole to the neighboring site is disturbed by the electrostatic potential produced by the ordered holes, which results in an abrupt increase of electrical resistance as well as a suppression of susceptibility. However, no anomalism presents in electrical resistance around the temperature (in Fig. 2), and reversely the susceptibility-value is increased below the temperature [in Fig. 5(d)]. So the assumption could be abstained, and the focus might be on the spins, etc. that significantly influence the magnetic properties only. It is reasonable to recall the theory proposed for the magnetic system by Griffiths[18] and

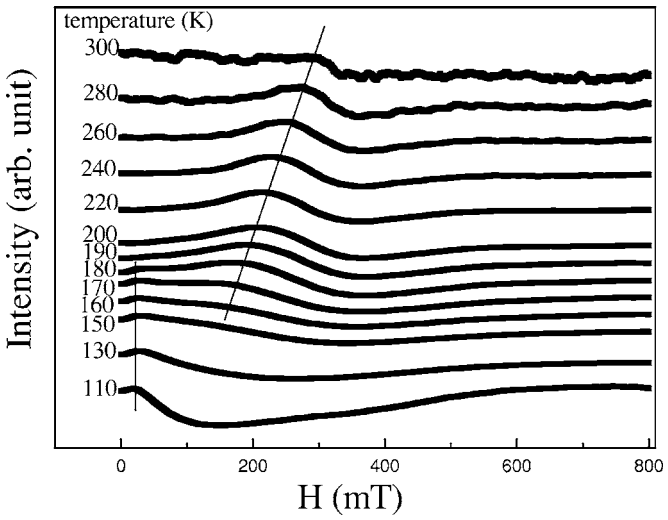

FIG. 7. ESR spectra of powder ceramic $Nd_{0.75}Sr_{1.25}CoO_4$ for a few representative temperatures.

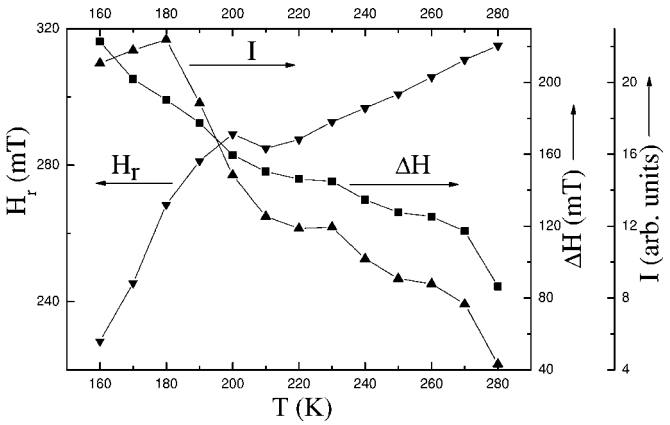

FIG. 8. Temperature dependence of the resonant field H_r, line width ΔH_{pp} and intensity I about the A signal.

Bray.[19] According to this theory, for a system with randomly distributed spins there is always a finite probability of ferromagnetic clusters in the paramagnetic background for the temperature range of $T_C < T < T_G$. Here T_G is called the Griffiths temperature, and the temperature range between T_G and T_C is termed as the Griffiths phase. Applying the Griffiths singularity, we will explain the anomalous behavior in the samples. The formation of ferromagnetic clusters cause a deviation of $\chi(T)$ from the Curie-Weiss form, as seen in Fig. 5(d). On the other hand, the ferromagnetic clusters within the paramagnetic matrix would lead to the magnetic heterogeneity, resulting in the anomalous paramagnetic behavior as observed in the ESR spectra parameters.

In summary, the structure, magnetic, and transport properties of $Nd_{1-x}Sr_{1+x}CoO_4$ ($x=0.25$, 0.33, and 0.60) are investigated. The specimens show semiconducting properties over all the temperature range measured and follow the Arrhenius law at high temperatures. Small polaron models may be applied to explain the transport mechanism of the material. Spin-glass states and Griffiths singularity are observed in susceptibility and electron spin resonance. The Sr doping in this system can intensely influence the samples' structure, electrical, and magnetic properties.

ACKNOWLEDGMENTS

This work is supported by the Natural Science Foundation of China (No. 10104013 and No. 50421201) and by the National Basic Research Program of China (No. 2006CB601003).

*Corresponding author. Telephone: +86-551-3600652; Fax: +86-551-3601073. Email address: kqruan@ustc.edu.cn

[1] Y. Moritomo, K. Higashi, K. Matsuda, and A. Nakamura, Phys. Rev. B **55**, R14725 (1997).
[2] G. J. Xu, Q. R. Pu, B. Liu, R. H. Tao, G. S. Wang, Z. J. Ding, J. C. Grivel, and N. H. Andersen, Phys. Rev. B **69**, 104506 (2004).
[3] Y. Moritomo, Y. Tomioka, A. Asamitsu, Y. Tokura, and Y. Matsui, Phys. Rev. B **51**, R3297 (1995).
[4] P. Mahadevan, K. Terakura, and D. D. Sarma, *Proceedings of the 4th Asian Workshop on First-Principles Electronic Structure Calculations*, Taipei, Taiwan (2001).
[5] L. M. Helme, A. T. Noothroyd, D. Prabhakaran, F. R. Wondre, C. D. Frost, and J. Kulda, Physica B **350**, 273 (2004).
[6] S. W. Cheong, H. Y. Hwang, C. H. Chen, B. Batlogg, L. W. Rupp, Jr., and S. A. Carter, Phys. Rev. B **49**, 7088 (1994).
[7] M. Sanchez-Andujar and M. A. Senaris-Rodriguez, Solid State Sci. **6**, 21 (2004).
[8] S. Castro-Garcia, M. Sanchez-Andujar, C. Rey-Cabezudo, M. A. Senaris-Rodriguez, and C. Julien, J. Alloys Compd. **323-324**, 710 (2001).
[9] J. Matsuno, Y. Okimoto, Z. Fang, X. Z. Yu, Y. Matsui, N. Nagaosa, M. Kawasaki, and Y. Tokura, Phys. Rev. Lett. **93**, 167202 (2004).
[10] X. L. Wang and E. Takayama-Muromachi, Phys. Rev. B **72**, 064401 (2005).
[11] J. B. Goodenough, J.-S. Zhou, and J. Chan, Phys. Rev. B **47**, 5275 (1993).
[12] X. Gaojie, M. Zhiqiang, J. Hao, Y. Hongjie, W. Bin, L. Dengpan, and Z. Yuheng, Phys. Rev. B **59**, 12090 (1999).
[13] K. Asai, P. Gehring, H. Chou, and G. Shirane, Phys. Rev. B **40**, 10982 (1989).
[14] Y. Shong-Liu, L. Sheng, C. Heng, S. Jing-Lin, D. Bo, X. Zheng-Cai, and L. Jian-Qing, Chin. Phys. Lett. **21**, 2285 (2004).
[15] Ch. Binek, W. Kleemann, and D. P. Belanger, Phys. Rev. B **57**, 7791 (1998).
[16] J. A. Mydosh, *Spin Glasses: An Experimental Introduction* (Taylor and Francis, London, 1993).
[17] V. A. Ivanshin, J. Deisenhofer, H.-A. Krug von Nidda, A. Loidl, A. A. Mukhin, A. M. Balbashov, and M. V. Eremin, Phys. Rev. B **61**, 6213 (2000).
[18] R. B. Griffiths, Phys. Rev. Lett. **23**, 17 (1969).
[19] A. J. Bray, Phys. Rev. Lett. **59**, 586 (1987).